

1 The potential of marine bivalve *Spisula sachalinensis*
2 as a marine temperature record

3 Tansy Branscombe^{a,*}, Rick Schulting^a, Julia Lee-Thorp^a, Melanie J. Leng^b

4 ^a*School of Archaeology, University of Oxford, 1 South Parks Road OX1 3TG*

5 ^b*National Environmental Isotope Facility, British Geological Survey, Nicker Hill,*
6 *Keyworth, Nottingham NG12 5GG and School of Biosciences, University of Nottingham,*
7 *Sutton Bonington Campus, Loughborough, LE12 5RD*

8 **Abstract**

9 This paper presents a four year subannual isotope marine temperature
10 record using modern *Spisula sachalinensis* specimens from Tomakomai (Hokkaido's
11 Pacific coast, Japan). This species is commonly found in pre- and protohis-
12 toric shell middens and faunal assemblages from around the Seas of Japan
13 and Okhotsk, so has significant potential as an indicator of (pre)historic ma-
14 rine and, by inference, climatic conditions. However, previous sclerochrono-
15 logical research on the species' growth has shown significant geographical
16 variation in growth pattern, rendering palaeoclimatic interpretation difficult.
17 To address this issue, this study applied sequential isotopic analysis on two
18 sectioned modern valves, providing a proxy for sea surface temperature (SST)
19 and allowing the direct identification of seasonality during shell growth. The
20 sequences span four years of growth, as confirmed by visually identified
21 growth patterns and the oxygen isotope results, which show clear annual
22 cycles in $\delta^{18}\text{O}$. $\delta^{13}\text{C}$ seasonality is less clear, but shows a weak inverse corre-
23 lation with temperature potentially relating to primary productivity. Annual
24 growth lines show that shell growth occurs during both warm and cooler SST,
25 but is more rapid during the cooler seasons. This is consistent with warm-
26 season growth minima seen in shells from Hakodate Bay by Kato and Hamai
27 (1975), but not with their suggestion that it is associated with shells grow-
28 ing at the southern limits of their distribution. Comparison to average local
29 SST shows that $\delta^{18}\text{O}$ -derived temperature falls within the expected range,
30 but, contrary to expectations given preferential cool-season shell growth, ap-
31 pears biased towards warmer temperatures. Factors that could contribute to
32 this are discussed. Overall, stable isotope analysis of *Spisula sachalinensis*

*Corresponding author

Email addresses: `tansy.branscombe@arch.ox.ac.uk` (Tansy Branscombe),
`rick.schulting@arch.ox.ac.uk` (Rick Schulting), `julia.lee-thorp@arch.ox.ac.uk`
(Julia Lee-Thorp), `mjl@bgs.ac.uk` (Melanie J. Leng)

is considered a useful complement to macro/microscopic sclerochronological research in building a holistic picture of shell growth, and has significant potential as a high resolution proxy for palaeoenvironmental studies of past SST.

Keywords:

Palaeoclimate, Northwest Pacific, Oxygen isotopes, Sclerochronology, Seasonality

1. Introduction

The value of marine bivalve shells as temperature archives has long been recognised (e.g. Emiliani et al., 1964), with high resolution sampling and increasingly precise stable isotope mass spectrometry allowing the interpretation of data at subannual scales. Following the recognition that some species of clam, e.g. *Arctica islandica*, can live for more than 500 years (Butler et al., 2013; Schöne et al., 2005), researchers have noted the importance of long-lived molluscs as ‘sentinel species’ in marine climate research (Mann et al., 2013). The shells of such large clams grow incrementally allowing for correlation between annual growth increments and calendar dates (e.g. Khim et al., 2000). Furthermore, their shell oxygen and carbon stable isotope ratios ($\delta^{18}\text{O}_{\text{shell}}$ and $\delta^{13}\text{C}_{\text{shell}}$) reflect information about ambient water conditions. Water temperature and salinity in particular drive $\delta^{18}\text{O}_{\text{shell}}$, while $\delta^{13}\text{C}_{\text{shell}}$ has a more complicated relationship to water conditions involving animal metabolic effects, salinity and dissolved inorganic carbon (DIC) (McConnaughey and Gillikin, 2008). This means that the growth increments can be interpreted as subannual proxy records for these variables (Emiliani et al., 1964).

Spisula (*Macra/Pseudocardium*) *sachalinensis* (Figure 1), or the Sakhalin surf clam, is a large bivalve found in the Northwest Pacific, notably in Japan, the Korean peninsula and the Russian Far East (including the eponymous Sakhalin Island). In Japanese this species is known as ubagai (ウバガイ) or hokkigai (ホッキ貝). It is easily recognised by its bright pink muscle and is eaten both raw and cooked. The majority of Japanese surf clam harvest occurs from the port city of Tomakomai on the south coast of Hokkaido (Figure 2), where clams are dredged using jet stream seine fishing. As of 1999, 50,000 tons of clam were caught from the Tomakomai coast annually, and it remains a specialty dish of the region (Sasaki and Ohta, 1999).

Previous research on the species has been guided by its commercial im-

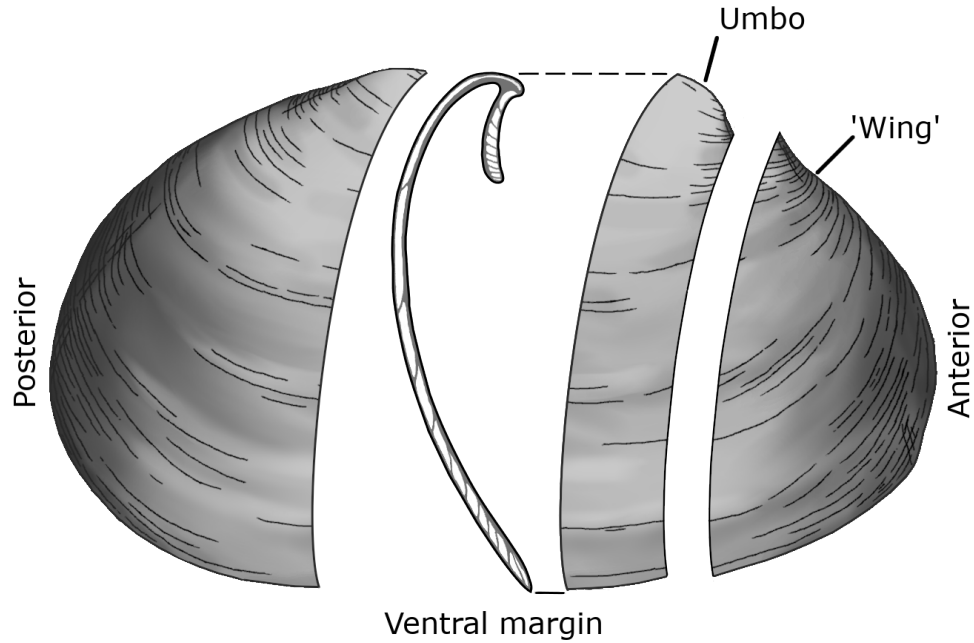


Figure 1: Schematic illustration of *Spisula sachalinensis* showing section along the axis of maximum growth

portance, focusing on its nutritional value and optimal growth and spawning conditions (e.g. Golikov and Scarlato, 1970; Kato and Hamai, 1975; Lee et al., 1996; Sakurai and Seto, 1998; Sasaki, 1981; Sasaki and Ohta, 1999; Tabakaeva and Tabakaev, 2017; Takahashi and Yamamoto, 1970).

The potential of this species for climate science has not gone unrecognised. For example Mann et al. (2013) list it as one of four major long-lived mactrid clam species, and note that the genus *Spisula* has been suggested as a good continental shelf sentinel species covering both the North Pacific and North Atlantic. The only isotopic study to specifically test the species as a climatic indicator, however, is that by Khim et al. (2000), confirming the expected relationship between $\delta^{18}\text{O}_{\text{shell}}$ and sea surface temperature in specimens from the east coast of Korea. They also discuss trends in $\delta^{13}\text{C}_{\text{shell}}$, suggesting that as in other bivalve species (e.g. Gillikin et al., 2006; McConnaughey and Gillikin, 2008) this is primarily a reflection of the $\delta^{13}\text{C}$ of DIC.

Khim et al. (2000) focus on the utility of *S. sachalinensis* as a monitor for modern hydrological conditions, but do briefly mention possibilities for palaeoclimatic research.

Our study continues this research, but focuses on the region of Hokkaido as opposed to the Korean coast. Not only is this region notable for the modern commercial harvest of *S. sachalinensis* as previously outlined, it is also an important area for Japanese archaeology. In Hokkaido, unlike in central/southern Japan, coastally-

adapted indigenous hunter-gatherers remained the primary occupants into the late 19th century (Hudson, 2014; Ohnuki-Tierney, 1976; Seaton, 2017). The maritime adaptations of Jomon, Epi-Jomon, Okhotsk and Ainu groups - representing a span of c. 7000 years - mean that shell middens are a frequent element of the archaeological record in Hokkaido (Habu et al., 2011; Oikawa, 1995; Okada, 1998), and the surf clam is a common species found at sites in northern Japan and Hokkaido (Makino, 2011; Nagasaki, 1994; Okada, 1998). Use of the species as a palaeothermometer could provide an important sub-annual oceanographic and palaeoclimatic proxy, given the interdependence of oceanographic and atmospheric factors and their effect on regional SST (e.g. Abe et al., 2016; Hirose and Ichi Fukudome, 2006; Imada et al., 2017; Seo et al., 2013; Takano et al., 2008).



Figure 2: Map showing the location of Tomakomai within northern Japan, and the surrounding ocean currents.

121 For Honshu and the southern islands of Japan much of the historical
 122 period is well-documented climatically by instrumental measurements (back
 123 to the late 18th century (Demaree et al., 2013; Können et al., 2003)) and
 124 historical documents (back to the 11th century(Mikami, 2008)). However,
 125 as Hokkaido was not colonised by the Japanese state until after the Meiji
 126 restoration of 1868 there is relatively little historical climatic documenta-
 127 tion that specifically relates to this region. Therefore, the use of shellfish
 128 (and other marine carbonates) have the potential to fill significant gaps in
 129 archaeological and palaeoclimatic knowledge, both due to their archaeologi-
 130 cal prevalence and the relative gap in historical climatic data specific to this
 131 island.

132 We aim to use high-resolution analysis of $\delta^{18}\text{O}_{\text{shell}}$ and $\delta^{13}\text{C}_{\text{shell}}$ to iden-
 133 tify seasonality of growth through isotope analysis of a modern, known-age
 134 *S. sachalinensis*. A focus is placed on identifying the season of growth de-
 135 crease/cessation, which has been a point of disagreement in previous research,
 136 as outlined below. We aim to investigate the relationship between $\delta^{18}\text{O}_{\text{shell}}$
 137 and sea surface temperature, in order to demonstrate the potential of *S.*
 138 *sachalinensis* for palaeoclimatic reconstruction in the Northwest Pacific.

139 2. Growth and ecology

140 *S. sachalinensis* is a species that prefers sandy substrates in the littoral
 141 zone, growing rapidly for c. eight years, when shell length reaches its maxi-
 142 mum size of around 10 cm in length and subsequent growth becomes negligi-
 143 ble (Sasaki, 1981). Large shells are often 20-30 years old, with one individual
 144 from the Sea of Japan even reported to have reached 70 years (Selin, 2010).
 145 The species reaches sexual maturity at three years (Golikov and Scarlato,
 146 1970), after which spawning takes place annually during the spring/early
 147 summer in Hokkaido (Kinoshita and Shibuya, 1920; Sakurai et al., 1992;
 148 Sasaki, 1981; Takamaru, 1976). In Primorje, Russian Far East, Golikov and
 149 Scarlato (1970) report spawning between late June and October. It seems
 150 likely that these differences relate to temperature variation between regions,
 151 as Lee et al. (1996) have shown that water temperature can be a limiting
 152 factor for egg development in *S. sachalinensis*.

153 Water depth estimates for living colonies vary from 1-5 m (Golikov and
 154 Scarlato, 1970), to 3-6 m (Sasaki and Ohta, 1999) and up to 12-15 m (Sasaki,
 155 1989). Golikov and Scarlato (1970) discuss seasonal change in depth distri-
 156 bution, although the extent of this variation does not account for the wide

157 differences in depth range described in the literature. Sasaki (1989) suggests
158 that a maximum depth of 15 m is common across a number of fishing spots,
159 as a result of sediment conditions. Coarser-grained sand particles found
160 at greater depths inhibit the shellfish's burrowing behaviour. Differences
161 in sediment composition across the species' geographical distribution could
162 therefore be responsible for different depth ranges given in the literature.

163 As is common in marine bivalves, growth is not constant throughout
164 the year, resulting in the formation of annual growth increments and lines
165 (Kato and Hamai, 1975; Sasaki, 1981). Growth increments show a prismatic
166 structure and represent rapid shell growth. Growth lines are a nacreous layer
167 (due to a difference in the orientation of the crystal structure or the organic
168 compounds therein) and represent a period of slowed or ceased shell growth
169 (Kato and Hamai, 1975). Both of these layers are composed of aragonite
170 (CaCO_3). In *S. sachalinensis*, previous work suggests three potential triggers
171 for the formation of annual growth lines: low winter SST (Yamamoto, 1947),
172 high summer SST (Sasaki, 1981) and the end of the spawning season (Kato
173 and Hamai, 1975). As with variation in spawning season, it seems likely that
174 these multiple triggers relate to different environmental conditions across the
175 species' geographic distribution; the warm-season growth lines reported by
176 Sasaki (1981) occurred in shells near the southern end of the *S. sachalinensis*
177 distribution in Sendai Bay, Honshu, whereas the cool-season lines reported
178 by Yamamoto (1947) were from its northern distribution on Sakhalin. Given
179 the expected relationship between $\delta^{18}\text{O}_{\text{shell}}$ and SST, stable isotope analysis
180 of a modern specimen of *S. sachalinensis* from Tomakomai should confirm
181 the species' regional growth pattern.

182 3. Materials and methods

183 The modern shells used in this study were collected from the coast of
184 Tomakomai on Hokkaido's Pacific coast (Figure 2) in August 2019.

185 The shells were obtained from a Sapporo sushi restaurant, and had been
186 briefly boiled (<20 minutes) by the restaurant to remove any remaining or-
187 ganic material before export to the UK (standard practice as required by the
188 UK Department for Environment Food & Rural Affairs). As these shells were
189 obtained from a restaurant rather than directly from the study site, we are
190 not able to provide exact coordinates, however the restaurant confirm that
191 they were harvested in Tomakomai on 3rd August 2019 at approximately
192 42°35'N, 141°36'E.

193 Age estimate of the two shells were obtained via preliminary identification
194 of annual growth lines, which were later confirmed or adjusted based on the
195 shells' $\delta^{18}\text{O}_{\text{shell}}$ profiles. One specimen (TBMOD1) is estimated to have been
196 28 years old at the time of collection, and the other (TBMOD2) is estimated
197 at 26 years old. From this assessment, the four years sampled in this study
198 are considered most likely to represent 1996-1999 (Figure 3).

199 Shells were sectioned using a geological trim saw with a 15.24 cm diameter
200 diamond saw blade of 0.1 cm thickness. They were sectioned from the umbo
201 to the shell edge by manually holding the shell in position along the axis
202 of maximum growth, perpendicular to growth banding (Figure 1). After
203 sectioning, the 'wing' on the anterior side was also cut away to leave a thick
204 section. Sections were embedded with the cut surface corresponding to the
205 axis of maximum growth face down in a plastic mould. using MetPrep 'Kleer-
206 Set' polyester resin and hardener, and were left to cure overnight. Once fully
207 cured, the side representing the axis of maximum growth was prepared using
208 a series of silicon carbide grinding and polishing papers. These ranged from
209 P180 up to P4000, producing a polished sampling surface and ensuring that
210 no resin residue remained over the sampling area.

211 Resin blocks were mounted onto the sampling slide of a New Wave Re-
212 search microdrill. This allows for high resolution computer-controlled drilling
213 of the growth bands. A 0.3 mm diamond-coated dental drill bit was fitted
214 to the micromill to sample incrementally across the shell section. A section
215 of growth encompassing three annual growth bands was selected for each
216 shell (Figure 3). This came from the middle of the shell's growth, when the
217 shell is growing fast enough to provide wide increments but not from the
218 earliest years of growth when the outer shell layer being targeted is thinner.
219 The distance between samples (measured from the centre of one sample to
220 the centre of the next) averaged 0.8 mm. The samples that coincided with
221 nacreous growth lines were specifically noted. Samples were drilled over three
222 passes at 100 μm depth per pass (300 μm total depth), with a scan speed of
223 100 $\mu\text{m}/\text{second}$. A total of 37 samples of aragonite powder were produced,
224 and these each weighed around 50 μg .

225 Further samples were hand drilled from each shell to test for diagenetic
226 alteration of the aragonite. These were analysed using FTIR-ATR, using
227 the method outlined by Loftus et al. (2015), which differentiates aragonite
228 and calcite polymorphs using the different vibrational characteristics of their
229 molecular structure. Results showed no evidence of aragonite-to-calcite re-
230 crystallisation, but the work of Moon et al. (2018) suggest that a lack of

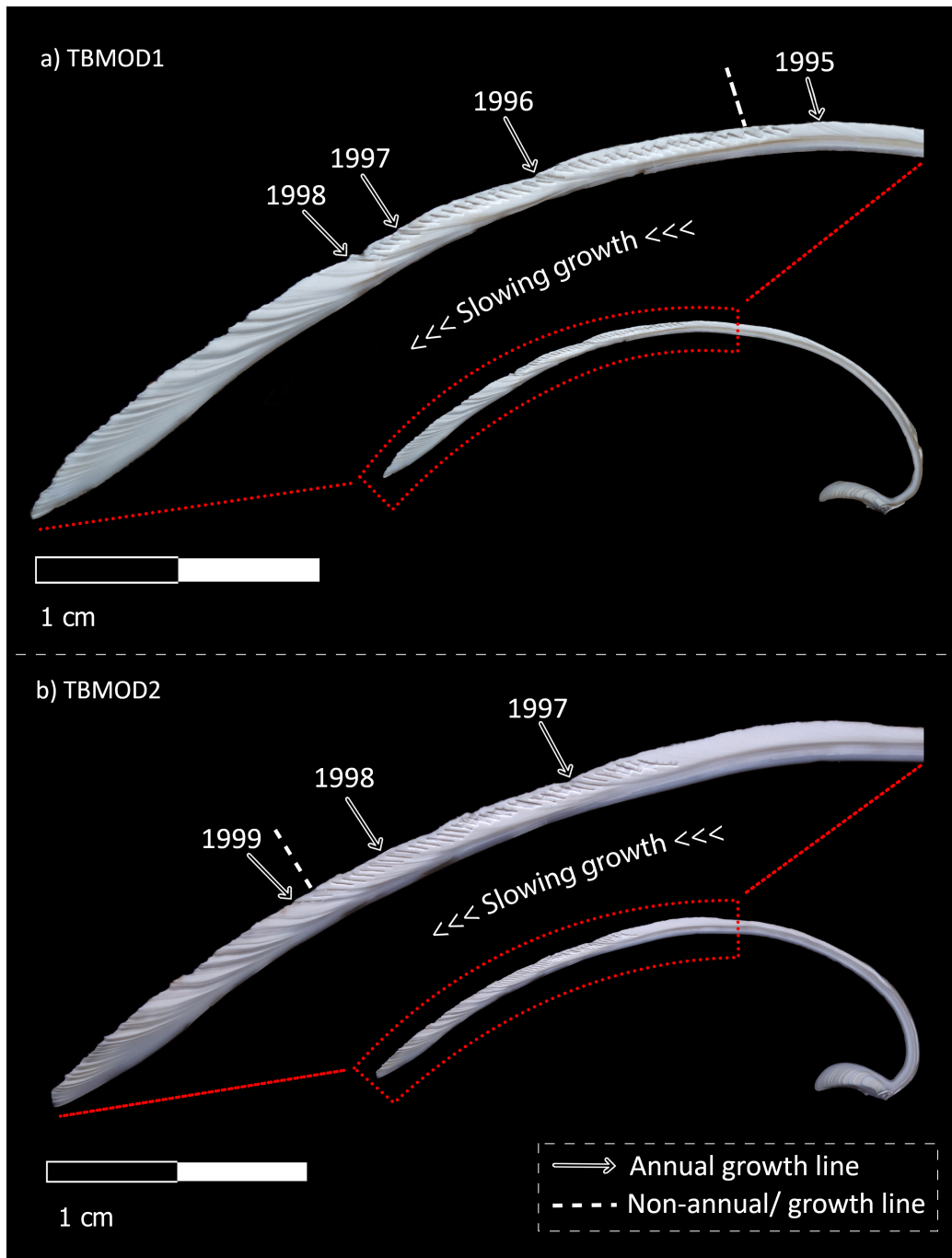


Figure 3: Image of sectioned *Spisula sachalinensis* valves showing completed micromill sampling and the location of growth lines. NB: the non-annual growth line marked by a dashed line in TBMOD1 has been partially obscured by the milling tracks.

231 calcite recrystallisation does not preclude diagenetic shifts in $\delta^{18}\text{O}_{\text{shell}}$.

232 Isotope ratio mass spectrometry was undertaken at the British Geolog-
233 ical Survey in Keyworth, using an IsoPrime dual inlet mass spectrometer
234 and Multiprep device. Sample isotope values are reported using the delta
235 notation ($\delta^{18}\text{O}$, $\delta^{13}\text{C}$) in per mil, calculated on the VPDB scale using a lab-
236 oratory standard calibrated against NBS-19. Nine calcite standards (KCM)
237 were measured alongside every 31 samples. A calcite-acid fractionation fac-
238 tor, Craig correction (Craig, 1957), and drift correction (measured using
239 standards at the start and end of the run) were applied to all measurements.
240 The average analytical precision for KCM standards run at the same time
241 was $\pm 0.05\text{‰}$ for $\delta^{18}\text{O}$ and $\pm 0.03\text{‰}$ for $\delta^{13}\text{C}$. An uncertainty of $\pm 0.05\text{‰}$
242 $\delta^{18}\text{O}$ would in turn correspond to an error of $\pm 0.24\text{ °C}$ in the reconstruc-
243 tion of water temperature at the time of formation, using the aragonite-SST
244 equation:

$$SST = 20.6 - 4.34(\delta^{18}\text{O}_{\text{carbonate}} - (\delta^{18}\text{O}_{\text{seawater}} - 0.27)) \quad (1)$$

245 This is a slightly modified version of the original (Grossman and Ku, 1986)
246 equation, where a -0.27‰ correction has been applied to the seawater $\delta^{18}\text{O}$
247 value ($\delta^{18}\text{O}_{\text{seawater}}$) to account for measurmenets on the modern VSMOW
248 (Vienna Standard Mean Oceanic Water) scale rather than the now-defunct
249 SMOW scale originally used (Dettman et al., 1999; Leng and Lewis, 2016).
250 $\delta^{18}\text{O}_{\text{seawater}}$ was set at a constant -0.85‰ , based on data from NASA’s
251 Global Seawater Oxygen-18 Database (Schmidt et al., 1999) (<https://data.giss.nasa.gov/o18data/>).
252

253 The modern observed SST range for the Tomakomai coast was accessed
254 using the Physical Oceanography Distributed Active Archive Centre (PO-
255 DAAC) satellite imagery database. Specifically, we used Level 4 data from
256 the Canadian Meterological Center, which provides daily global SST mea-
257 surements at a 0.2 degree resolution, combining infrared imagery with in-situ
258 readings from ships and buoys to provide an estimate of foundation tempera-
259 ture, ‘defined as the temperature of the water column just below the diurnal
260 warm layer’ (Marullo et al., 2016, pg. 8357). While several global satel-
261 lite SST datasets exist within the Group for High Resolution Sea Surface
262 Temperature (GHR SST), this particular dataset was the only one at Level 4
263 resolution to provide the required data through the 1990s. The *ghrsst* Python
264 package developed for this work (Stuart, 2020) was used to access daily SST
265 observations from the Tomakomai coast, from January 1992 to December

266 2002. From this, monthly averages were calculated (Table 1) to provide a
267 general picture of the observed temperature range contemporary with the
268 sampled period of shell growth. The range in average monthly temperature
269 is 17.43 °C, while the maximum average annual temperature range (the dif-
270 ference between the average February minimum and August maximum) is
271 18.93 °C.

Table 1: Summary of average monthly observed SST (°C) for the Tomakomai coast for the period of 1992-2002. Daily readings were used to produce a minimum, maximum and mean reading for each month, which were then averaged over all years of available data. Raw data at: <https://podaac-opendap.jpl.nasa.gov/opendap/hyrax/allData/ghrsst/data/GDS2/L4/GLOB/CMC/CMC0.2deg/v2/contents.html>

	Jan	Feb	Mar	Apr	May	Jun	Jul	Aug	Sep	Oct	Nov	Dec
Average Min	3.40	2.27	2.38	3.16	5.79	10.55	14.72	19.21	17.82	13.43	9.26	5.68
Average	4.66	2.97	3.01	4.38	8.01	12.72	17.14	20.40	19.47	15.66	11.11	7.41
Average Max	6.03	3.01	3.71	5.86	10.36	14.87	19.36	21.20	21.20	17.79	13.26	9.27

272 4. Results

273 Of the 78 samples analysed for isotope composition, seven failed to pro-
274 duce enough gas for isotopic measurement. Isotope data are shown in Table
275 2. $\delta^{18}\text{O}_{\text{shell}}$ shows a range of 3.46‰, while $\delta^{13}\text{C}_{\text{shell}}$ range is 1.55‰. Lin-
276 ear regression analysis shows a weak and statistically insignificant negative
277 correlation between $\delta^{18}\text{O}_{\text{shell}}$ and $\delta^{13}\text{C}_{\text{shell}}$ ($r = -0.18$, $p = 0.14$). $\delta^{18}\text{O}_{\text{shell}}$
278 results equated to a temperature range of 15.01 °C, with a minimum of 5.40
279 °C and a maximum of 20.41 °C (Table 2).

280 The stable isotope data (Figure 4) show clear peaks and troughs in
281 $\delta^{18}\text{O}_{\text{shell}}$ in three cycles, matching the expected three-year sampling peri-
282 ods. In general the $\delta^{18}\text{O}_{\text{shell}}$ peaks appear broader than the corresponding
283 troughs, leading to a ‘cusplate’ rather than sinusoidal wave appearance, as
284 defined by Goodwin et al. (2003). As samples move towards the ventral
285 growth edge (Figure 1) the periodicity of the wave decreases, corresponding
286 to shortening growth increments.

287 Figure 5 shows SST calculations from $\delta^{18}\text{O}_{\text{shell}}$ overlain on observed SST
288 variation for Tomakomai, illustrating how the $\delta^{18}\text{O}_{\text{shell}}$ -derived temperatures
289 fit against observed annual SST range for the local coast. In fig. 5, the

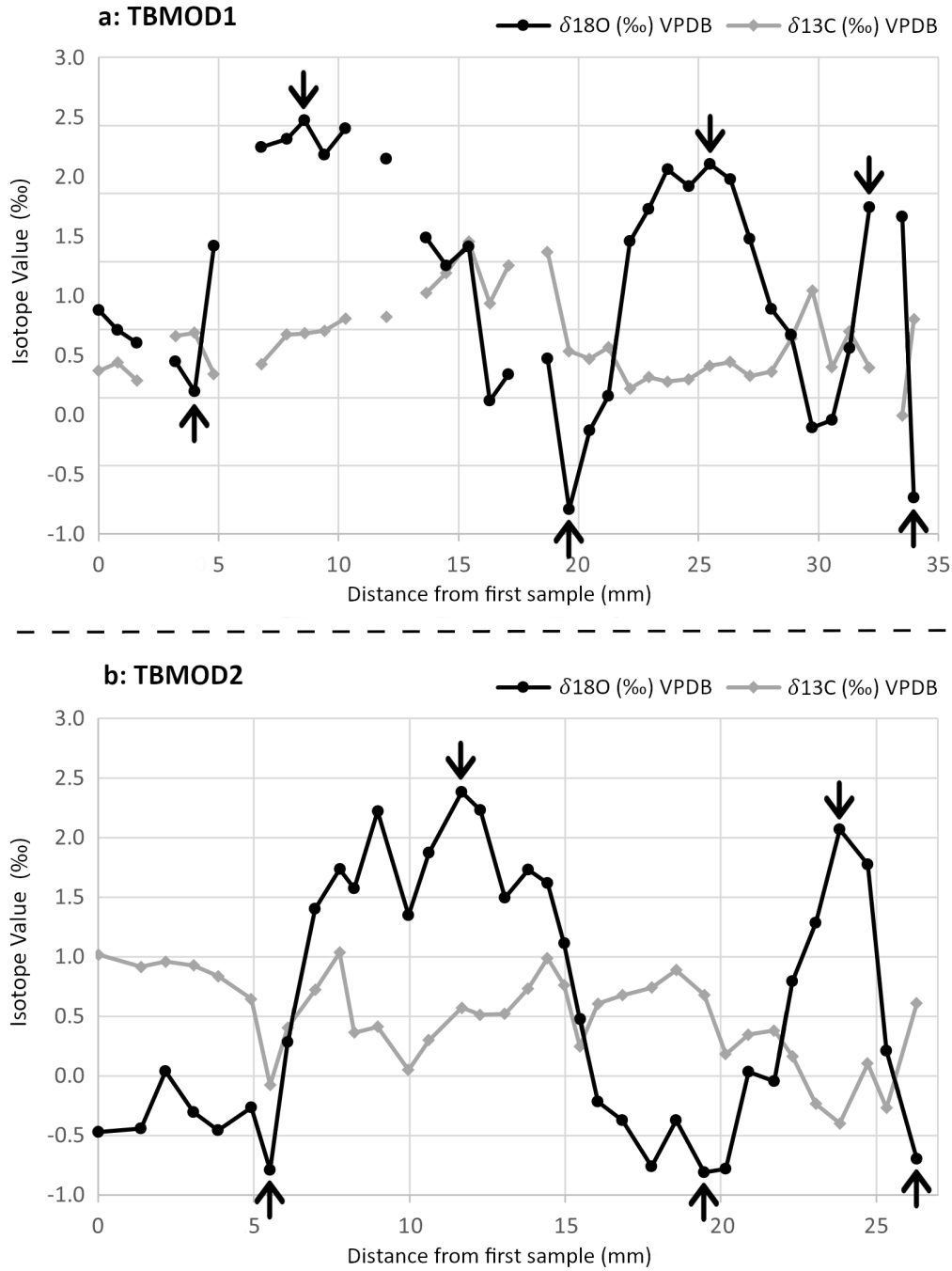


Figure 4: Graph plotting oxygen and carbon stable isotope results. Peaks and troughs in $\delta^{18}\text{O}_{\text{shell}}$ marked with arrows. Earliest/closest to umbo shell growth on the left.

Table 2: Stable isotope data from shells TBMOD1 and TBMOD2 alongside $\delta^{18}\text{O}_{\text{shell}}$ -derived sea surface temperature (SST). Failed samples are greyed out. SST calculations have an uncertainty of ± 0.24 °C due to analytical precision based on the aragonite-SST conversion defined in eq. (1).

Number	Sample ID	$\delta^{18}\text{O}$ (‰) VPDB	$\delta^{13}\text{C}$ (‰) VPDB	SST (°C)	Comments
1	TBMOD1-101	+0.64	+0.20	13.0	
2	TBMOD1-102	+0.50	+0.26	13.6	
3	TBMOD1-103	+0.40	+0.13	14.0	
4	TBMOD1-104	NA	NA	NA	Growth stoppage
5	TBMOD1-105	+0.26	+0.45	14.6	
6	TBMOD1-106	+0.05	+0.48	15.5	
7	TBMOD1_1	NA	NA	NA	
8	TBMOD1_2	+1.12	+0.17	10.9	
9	TBMOD1_3	NA	NA	NA	Growth stoppage
10	TBMOD1_4	+1.84	+0.25	7.8	
11	TBMOD1_5	+1.90	+0.46	7.5	
12	TBMOD1_6	+2.04	+0.47	6.9	
13	TBMOD1_7	+1.78	+0.49	8.0	
14	TBMOD1_8	+1.98	+0.58	7.2	
15	TBMOD1_9	NA	NA	NA	
16	TBMOD1_10	+1.75	+0.59	8.1	
17	TBMOD1_11	NA	NA	NA	
18	TBMOD1_12	+1.18	+0.77	10.6	
19	TBMOD1_13	+0.97	+0.92	11.5	
20	TBMOD1_14	+1.11	+1.15	10.9	
21	TBMOD1_15	-0.02	+0.69	15.8	
22	TBMOD1_16	+0.17	+0.97	15.0	
23	TBMOD1_17	NA	NA	NA	
24	TBMOD1_18	+0.28	+1.07	14.5	
25	TBMOD1_19	-0.82	+0.34	19.3	Growth stoppage
26	TBMOD1_20	-0.24	+0.28	16.8	
27	TBMOD1_21	+0.01	+0.37	15.7	
28	TBMOD1_22	+1.15	+0.07	10.8	
29	TBMOD1_23	+1.38	+0.15	9.7	
30	TBMOD1_24	+1.68	+0.12	8.5	
31	TBMOD1_25	+1.55	+0.14	9.0	
32	TBMOD1_26	+1.71	+0.23	8.3	
33	TBMOD1_27	+1.60	+0.26	8.8	
34	TBMOD1_28	+1.17	+0.16	10.7	
35	TBMOD1_29	+0.65	+0.19	12.9	
36	TBMOD1_30	+0.46	+0.43	13.7	
37	TBMOD1_31	-0.22	+0.79	16.7	

38	TBMOD1_32	-0.16	+0.22	16.5	Growth stoppage
39	TBMOD1_33	+0.37	+0.48	14.2	
40	TBMOD1_34	+1.40	+0.22	9.7	
41	TBMOD1_35	NA	NA	NA	
42	TBMOD1_36	+1.33	-0.13	10.0	
43	TBMOD1_37	-0.74	+0.58	18.9	Growth stoppage
44	TBMOD2-1	-0.47	+1.02	17.8	
45	TBMOD2-2	-0.44	+0.91	17.7	
46	TBMOD2-3	+0.04	+0.96	15.6	
47	TBMOD2-4	-0.30	+0.93	17.1	
48	TBMOD2-5	-0.45	+0.84	17.7	
49	TBMOD2-6	-0.26	+0.65	16.9	
50	TBMOD2-7	-0.79	-0.08	19.2	Growth stoppage
51	TBMOD2-8	+0.28	+0.41	14.5	
52	TBMOD2-9	+1.40	+0.72	9.7	
53	TBMOD2-10	+1.73	+1.04	8.2	
54	TBMOD2-11	+1.57	+0.36	8.9	
55	TBMOD2-12	+2.22	+0.41	6.1	
56	TBMOD2-13	+1.35	+0.05	9.9	
57	TBMOD2-14	+1.87	+0.30	7.6	
58	TBMOD2-15	+2.38	+0.57	5.4	
59	TBMOD2-16	+2.23	+0.51	6.1	
60	TBMOD2-17	+1.50	+0.52	9.2	
61	TBMOD2-18	+1.73	+0.74	8.2	
62	TBMOD2-19	+1.62	+0.99	8.7	
63	TBMOD2-20	+1.11	+0.77	10.9	
64	TBMOD2-21	+0.48	+0.25	13.7	
65	TBMOD2-22	-0.21	+0.61	16.7	
66	TBMOD2-23	-0.37	+0.68	17.4	
67	TBMOD2-24	-0.76	+0.74	19.0	
68	TBMOD2-25	-0.37	+0.89	17.4	
69	TBMOD2-26	-0.81	+0.68	19.2	Growth stoppage
70	TBMOD2-27	-0.78	+0.18	19.1	Growth stoppage
71	TBMOD2-28	+0.04	+0.35	15.6	
72	TBMOD2-29	-0.04	+0.38	15.9	
73	TBMOD2-30	+0.80	+0.16	12.3	
74	TBMOD2-31	+1.29	-0.23	10.2	
75	TBMOD2-32	+2.07	-0.40	6.8	
76	TBMOD2-33	+1.78	+0.10	8.0	
77	TBMOD2-34	+0.21	-0.27	14.8	
78	TBMOD2-35	-0.70	+0.61	18.8	
79	TBMOD2-36	-1.08	-0.09	20.4	Growth stoppage
MIN		-1.08	-0.40	5.4	
MAX		+2.38	+1.15	20.4	
RANGE		3.46	1.55	15.0	
AVERAGE		+0.70	+0.45	12.7	

290 $\delta^{18}\text{O}_{\text{shell}}$ -derived SST results have been normalised to account for this slowing
 291 growth (and therefore decreasing width in annual growth increments) using
 292 a piecewise constant dilation factor. The distance between samples within a
 293 growth increment was multiplied by *maximum increment width/width of par-*
 294 *ticular growth increment*. This means that each year of growth appears equal
 295 in length, whilst maintaining the original relative spacing between samples
 296 within each increment. This was then placed over the satellite-observed SST
 297 curve for the relevant years to provide the best visual fit.

298 5. Discussion

299 5.1. How well does $\delta^{18}\text{O}_{\text{shell}}$ data match modern SST observations?

300 Overall, it is clear that estimates of SST based on $\delta^{18}\text{O}_{\text{shell}}$ follow a broadly
 301 sinusoidal pattern, and none fall outside of the observed range for the col-
 302 lection location. This reinforces the conclusion of Khim et al. (2000), that
 303 $\delta^{18}\text{O}_{\text{shell}}$ in *S. sachalinensis* can be interpreted as a proxy for subannual
 304 cycling of marine temperatures. The results in fig. 4 show shortening pe-
 305 riod in the later years of shell growth, in keeping with expectations from the
 306 ecological literature for *S. sachalinensis*, which suggests significantly slowed
 307 growth after individuals reach ~eight years (Sasaki, 1981).

308 Due to the nature of shell growth, as well as the sampling methodology
 309 used, some ‘dampening’ of the true seasonal signal (Goodwin et al., 2003)
 310 is to be expected in such proxies; although micromill sampling resolution is
 311 high compared to other techniques, it will still result in some averaging over
 312 the true extremes in $\delta^{18}\text{O}_{\text{shell}}$, which is exacerbated by decreasing increment
 313 width as a shell’s ontological age increases. We can see this ‘dampening’
 314 effect in these results, with a calculated temperature range of 15.01 °C, while
 315 the range for average observed SST range was higher at 17.43 °C. The overall
 316 average temperature across the observed satellite data was 10.62 °C, while the
 317 average of the $\delta^{18}\text{O}_{\text{shell}}$ -derived SST calculations is two degrees higher at 12.7
 318 °C. Nonetheless, we can observe a good fit between observed and calculated
 319 temperatures, particularly in the overall shape of the temperature curve and
 320 around the seasonal peaks in SST. As will be discussed in Section 4.3, this
 321 bias towards warmer temperatures and poorer fit around SST minima is
 322 unexpected given the seasonality of growth line formation.

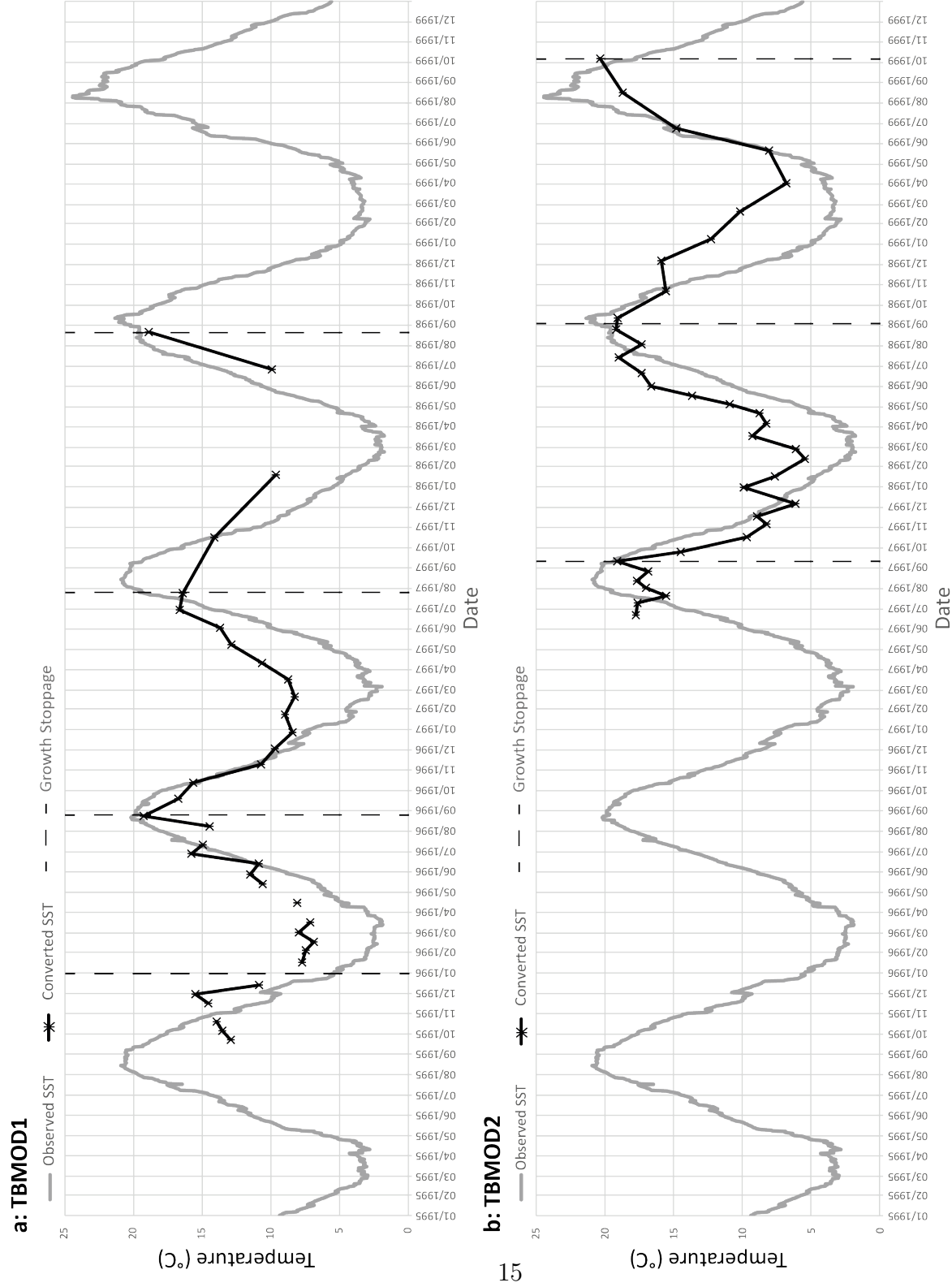


Figure 5: Temperature estimation based on $\delta^{18}\text{O}_{\text{shell}}$ results, overlain on average annual SST range for Tomakomai (table 1) where the annual period has been piece-wise linearly transformed to account for decreasing growth rate.

323 5.2. Interpretation of $\delta^{13}\text{C}_{\text{shell}}$ Results

324 Interpreting variation in $\delta^{13}\text{C}_{\text{shell}}$ values in marine carbonates is complex,
325 because it involves several interacting biological and chemical processes such
326 as surface productivity and dissolved carbon content, which in turn depend
327 on the particular oceanographic context in terms of (e.g.) thermocline depth,
328 prevailing currents, upwelling and salinity (Arthur et al., 1983a,b; Gillikin
329 et al., 2006; McConnaughey and Gillikin, 2008; ?). In this case, $\delta^{13}\text{C}_{\text{shell}}$
330 results show significantly less cyclicity than $\delta^{18}\text{O}_{\text{shell}}$, with a total amplitude
331 of just 1.55‰ (Figure 4), and a very weak negative correlation between
332 $\delta^{13}\text{C}_{\text{shell}}$ and $\delta^{18}\text{O}_{\text{shell}}$. This is similar to the findings of Khim et al. (2000),
333 who also see a smaller overall range and relative stability in $\delta^{13}\text{C}_{\text{shell}}$ compared
334 to $\delta^{18}\text{O}_{\text{shell}}$ for this species. They argue that this is related to the shallow
335 growth-depth of *S. sachalinensis*, which live primarily above the thermocline
336 and therefore do not record any major seasonal cycling in DIC. Although
337 we lack growth-depth information for the shells sampled here, we consider
338 that the situation is likely to be similar. The small degree of seasonal cycling
339 that is seen (slightly higher $\delta^{13}\text{C}_{\text{shell}}$ in the summer/autumn) could relate
340 to increased primary productivity and phytoplankton biomass in the warmer
341 season (Agboola et al., 2013). Overall though, the lack of in situ instrumental
342 records (e.g. DIC, salinity) from Tomakomai Bay, as well as detailed species-
343 specific information on the metabolism and physiological incorporation of
344 $\delta^{13}\text{C}$, prevents us from drawing more definitive conclusions on the potential
345 of $\delta^{13}\text{C}_{\text{shell}}$ as a palaeoenvironmental indicator in *S. sachalinensis*.

346 5.3. Potential confounding factors to $\delta^{18}\text{O}_{\text{shell}}$ interpretation

347 One of the main aims of this work was to identify the seasonality of growth
348 minima in *S. sachalinensis* from Tomakomai, as regular interruptions in shell
349 growth result in biased (towards the season of fastest growth) or incomplete
350 SST reconstructions. The ecological literature suggests that growth lines
351 can be triggered variously by excessively warm water (Sasaki, 1981), cold
352 water (Yamamoto, 1947) or by the end of the spawning season (Kato and
353 Hamai, 1975) which falls in spring/early summer for Hokkaido (Kinoshita
354 and Shibuya, 1920; Sakurai et al., 1992; Sasaki, 1981; Takamaru, 1976). In
355 this project, nacreous growth lines were identified during sampling so that the
356 samples representing these minima could be identified in the results. Based
357 on the relationship we have established between $\delta^{18}\text{O}_{\text{shell}}$ and SST, we can
358 use these results to identify when growth lines form in the seasonal growth
359 cycle.

360 The dashed lines in fig. 5 show the locations of growth lines identified
 361 during sampling. These data confirm that growth lines occurred on an annual
 362 basis, matching expectations from the literature. In all cases where the
 363 growth line sample yielded $\delta^{18}\text{O}$ data, that sample or one directly adjacent
 364 provided the annual peak in SST. This indicates that the growth lines form
 365 in later summer/autumn when SST is highest (table 1). This matches the
 366 findings of Sasaki (1981), who attributes this aestival growth interruption to
 367 shells located at the southern limits of the species' distribution. Our results
 368 show that an aestival growth minimum is not restricted to the southernmost
 369 distribution, and extends at least 500 km north of Sendai Bay to southern
 370 Hokkaido (the region of most importance for modern commercial harvesting).

371 For each shell sampled, there was one growth line identified that did not
 372 fit this warm-season growth pattern. These are labeled in fig. 3. On the ba-
 373 sis of the isotope results, we suggest that these represent non-annual growth
 374 interruptions. Although regular growth lines are expected to form due to
 375 predictable annual factors (e.g. seasonal SST, spawning), it is well known
 376 that other stressful events can also trigger the formation of growth lines in
 377 mollusc species. For example, Schöne (2008) notes that significant storms,
 378 or the exposure of shells during neap tides, can also cause this response. In
 379 this case, it is possible that a non-annual environmental stressor is responsi-
 380 ble for the growth line at sample three, which was then (mis)interpreted as
 381 an annually formed growth line. While it is not obvious from the satellite-
 382 observed record, it is worth noting that spring 1995 to spring 1996 was a La
 383 Niña event recorded in Japanese waters, indicating colder than average SST
 384 (http://ds.data.jma.go.jp/tcc/tcc/products/el_nino/ensoevents.html). A po-
 385 tential connection between non-annual growth interruptions and ENSO events
 386 in this region warrants further investigation. In cases with subannual sam-
 387 pling and clear seasonal cycling, we don't anticipate misinterpretation of
 388 non-annual growth interruptions will be an issue for palaeoenvironmental re-
 389 constructions based on isotope evidence, as the combination of macroscopic
 390 sclerochronology and $\delta^{18}\text{O}_{\text{shell}}$ allows for annual and exceptional growth lines
 391 to be differentiated.

392 If researchers were to target annual samples based on growth line anal-
 393 ysis of this species then misinterpretation of growth lines could result in
 394 errors where certain years are inadvertently sampled twice. This also poses
 395 a problem for the accurate aging of individual *S. sachalinensis* specimens,
 396 for example in this study the assignment of calendar years to the growth
 397 increments was carried out using a count of growth lines seen on the shell.

While the isotope results from the region of shell sampled meant that the non-annual lines identified could be factored into this assignment, it is certainly possible that further non-annual lines in the region of shell not sampled could also have been misinterpreted which would shift the calendar age of the sampled region. While none of the discussion in this study rests upon exactly accurate identification of the increments' calendar dates (excepting the possible connection between the non-annual growth line and 1995/6 La Niña event mentioned above), but in future research this is certainly an issue which should be examined closely and we suggest that where possible isotope analysis should supplement visual examination of growth lines to accurately identify whether they represent an annual growth stoppage.

Based on the positions of the growth lines in the $\delta^{18}\text{O}_{\text{shell}}$ cycle (aside from the exception outlined above), the shells grew preferentially in the cooler part of the year, with growth slowing or stopping completely during the warmest SSTs in late summer/autumn. By comparison to observed satellite data fig. 5, it appears that growth stoppage occurs during approx. August/September/October. This might suggest that $\delta^{18}\text{O}_{\text{shell}}$ would not reflect SST extremes during the warmer period of the year. As previously discussed, we would ordinarily expect some degree of 'dampening' of the seasonal temperature extreme from $\delta^{18}\text{O}_{\text{shell}}$, meaning that it is difficult to tell whether growth slows or stops completely during the formation of the growth line. In either case, we would expect that SST reconstruction would be biased towards the cooler part of the year. In practice, our results show annual SST minima consistently falling outside of the observed range and a minimum calculated SST at 6.9 °C compared to a satellite-observed minimum of 2.27 °C. This suggests that the isotope SST results are slightly offset from the observed satellite data towards warmer temperatures, which in turn means it is difficult to give a more precise estimate of the exact timing and duration of the growth stoppages. In explaining this offset, there are several potential contributing factors that we should consider, all of which are also more generally relevant in terms of the 'dampening' and palaeoclimatic interpretation of seasonal marine carbonate isotope proxies, as discussed below.

5.3.1. *Estimating $\delta^{18}\text{O}_{\text{seawater}}$*

As the other variable alongside $\delta^{18}\text{O}_{\text{shell}}$ in the aragonite palaeotemperature equation, misestimation of $\delta^{18}\text{O}_{\text{seawater}}$, as well as seasonally variable $\delta^{18}\text{O}_{\text{seawater}}$ has a significant impact on the accuracy of SST reconstructions. In modern cases such as this, the NOAA database can provide a regional

435 measurement, although this is not necessarily a close geographical match,
 436 and does not account for variation relating to seasonal currents or depth.
 437 In our data, for the difference between observed and calculated minimum
 438 SST to be accounted for by a misestimation of $\delta^{18}\text{O}_{\text{seawater}}$, the $\delta^{18}\text{O}_{\text{seawater}}$
 439 used would have needed to be at least $\sim 0.25\text{‰}$ lower (at -1.1‰). This would
 440 bring the average $\delta^{18}\text{O}_{\text{shell}}$ -derived SST down to $10.68\text{ }^{\circ}\text{C}$ and in line with
 441 the average SST observed from satellite data ($10.62\text{ }^{\circ}\text{C}$). A $\delta^{18}\text{O}_{\text{seawater}}$ value
 442 of -1.1‰ would be out of the expected range for the wider region; accord-
 443 ing to NASA data, within a c. 10 degree (lat/long) radius of Tomakomai
 444 bay, the minimum observed $\delta^{18}\text{O}_{\text{seawater}}$ was -0.89‰ . Furthermore, based on
 445 salinity data from the Japan Oceanographic Data Center (<https://data.giss.nasa.gov/cgi-bin/o18data>) and the salinity: $\delta^{18}\text{O}_{\text{seawater}}$ equation for
 446 the Tsushima current provided by Kodaira et al. (2016), we see that min-
 447 imum $\delta^{18}\text{O}_{\text{seawater}}$ is not reached until May, and total seasonal variation is
 448 only c. 0.4‰ . As the placement of the growth lines indicate warm-season
 449 growth interruptions, we would expect that the SST recorded in shell growth
 450 to be biased towards colder-season growth with an average temperature less
 451 than that of the observed data. To achieve this, an even larger reduction in
 452 $\delta^{18}\text{O}_{\text{seawater}}$ would be needed.

453
 454 Freshwater fluvial input is another consideration, and has the potential to
 455 affect coastal $\delta^{18}\text{O}_{\text{seawater}}$ values without necessarily impacting the measure-
 456 ments of the NOAA database which have been taken further from the shore.
 457 Tomakomai bay receives fluvial input from several minor rivers, the largest of
 458 which is the Yufutsu river, but unfortunately no $\delta^{18}\text{O}$ measurements appear
 459 to have been published relating to these inputs. Measurements of precipita-
 460 tion from Tomakomai provide an average annual $\delta^{18}\text{O}$ of -9.7‰ (Li, 2017). If
 461 shells were harvested from an area of the bay particularly affected by river-
 462 ine input then this could result in more negative $\delta^{18}\text{O}_{\text{seawater}}$ values than the
 463 -0.85‰ used in the palaeotemperature equation here which would help to ex-
 464 plain the temperature offset. Unfortunately, without more precise knowledge
 465 of the shell harvest location or in-situ measurements of near-shore $\delta^{18}\text{O}_{\text{seawater}}$
 466 we are unable to confirm that this is the case. This is therefore an avenue
 467 which should be further explored in future studies of this species and region.

468 5.3.2. Diurnal temperature variation

469 If extremes of temperature can inhibit shell growth on a seasonal basis, it
 470 follows that this could also affect growth on a daily basis if diurnal variation
 471 is regularly bringing seawater temperature outside of the preferred range.

472 This could also contribute to biases or ‘dampening’ in the proxy record. For
 473 the Tomakomai coast, diurnal warming (Δ SST) is expected to be small, with
 474 models predicting <1 °C Δ SST (Noh et al., 2011). This small variation is
 475 confirmed by comparing combined day- and night-time satellite SST data.
 476 Therefore, even if *S. sachalinensis* consistently precipitated preferentially
 477 during the warmest part of the day during the cooler months, this would not
 478 account for the offset in $\delta^{18}\text{O}_{\text{shell}}$ -derived winter temperatures.

479 5.3.3. Growth depth

480 In the other available paper addressing stable isotope results for *S. sacha-*
 481 *linensis*, the extent to which the full SST range was recorded varied between
 482 sampled individuals (Khim et al., 2000). The authors compare $\delta^{18}\text{O}_{\text{shell}}$ -
 483 derived SST range to observed SST (using the Grossman and Ku (1986)
 484 equation), although they do not present the specific SST calculations or
 485 specify the $\delta^{18}\text{O}_{\text{seawater}}$ value used. Nevertheless, they did not posit any
 486 species-wide offset in estimated SST and were confident in the use of *S.*
 487 *sachalinensis* as a SST proxy. Non-equilibrium precipitation is rare in ma-
 488 rine molluscs (McConnaughey and Gillikin, 2008; Twaddle et al., 2016), and
 489 it would be surprising in this species given that isotopic equilibrium has been
 490 shown for its Atlantic sibling, *S. solidissima* (Jones et al., 1983). Instead,
 491 Khim et al. (2000) suggest that the differences they observe could relate to
 492 the depth at which shells precipitated, although conflicting evidence exists
 493 as to whether shallower growth-depth corresponds to increased or decreased
 494 annual $\delta^{18}\text{O}_{\text{shell}}$ range (Geary et al., 1992; Krantz et al., 1987).

495 As this study is based on data from just two shells, and without de-
 496 tailed information on growth-depth, it is difficult to discuss the potential
 497 effects of this factor. Still, it is logical that growth-depth would signifi-
 498 cantly impact calculated SST, as variable temperature stratification in the
 499 top 10 metres of the water column may generate differences between growth-
 500 depth water temperature and foundation SST (Göttsche and Olesen, 2017)
 501 as modelled from satellite data. For example, Sakaizawa et al. (2018) show
 502 that for the Tomakomai coast the temperature at 5 m depth in February is
 503 ~ 0.5 °C warmer than the surface temperature. This magnitude of difference
 504 would go some, but not all the way to explaining the differences seen be-
 505 tween $\delta^{18}\text{O}_{\text{shell}}$ -derived SST results and observed cool-season temperatures.
 506 Increased species-specific understanding of the relationship between growth
 507 depth and $\delta^{18}\text{O}_{\text{shell}}$ would be also useful, especially for studies which discuss
 508 modern ecology or oceanography.

509 5.3.4. Sample treatment

510 Another possible explanation for anomalies seen in the proxy record could
 511 be the treatment of the samples after the shell collection that might lead to
 512 temperature offsets. Boiling of the shells is a potential concern for stable
 513 isotope analysis, as it has the potential to encourage isotopic exchange and
 514 so alter the original $\delta^{18}\text{O}_{\text{shell}}$ value. Milano et al. (2016) showed that for the
 515 aragonitic portion of gastropod *Phorcus turbinatus*, boiling at 100 °C did
 516 not produce significant isotopic exchange. They did see isotopic exchange
 517 in hotter temperatures (e.g. 300+ °C) and roasting conditions, but shifts in
 518 $\delta^{18}\text{O}_{\text{shell}}$ were also accompanied by visible changes in shell microstructure.
 519 Müller et al. (2017) suggested that $\delta^{18}\text{O}_{\text{shell}}$ may be slightly lowered by boil-
 520 ing, but do acknowledge that the differences seen between theirs and Milano
 521 et al.’s (2016) results were likely primarily due to experimental design. On
 522 the other hand, Moon et al. (2018) found that for *Spisula solidissima*, a
 523 shift in $\delta^{18}\text{O}_{\text{shell}}$ can occur even with ‘negligible’ mineralogical change and no
 524 calcite recrystallisation. This study looked at dry heat rather than boiling,
 525 but nonetheless raises the issue of heat-induced shifts in $\delta^{18}\text{O}_{\text{shell}}$, even for
 526 shells which appear to preserve seasonal cycling. For the shells used in this
 527 study, the length of boiling was <20 minutes, so significantly under the 40
 528 minutes used by Müller et al. (2017), and no changes in shell microstructure
 529 are visible to the naked eye.

530 Moon et al. (2018) suggest that isotopic exchange is possible even with-
 531 out visible change in shell microstructure, and according to Müller et al.
 532 (2017), boiling for 15 minutes can result in a change of -0.5‰ in $\delta^{18}\text{O}_{\text{shell}}$.
 533 In this study FTIR-ATR (attenuated total reflectance Fourier transform in-
 534 frared spectroscopy) was used to specifically check for recrystallisation of
 535 shell aragonite and no evidence was found. This means that extreme di-
 536 agenetic alteration (of aragonite into calcite) has not occurred, but there
 537 is still the possibility that a small but significant systemic shift in $\delta^{18}\text{O}_{\text{shell}}$
 538 could have occurred. Correcting for a -0.5‰ shift, as per Müller et al. (2017)
 539 would result in the $\delta^{18}\text{O}_{\text{shell}}$ -derived SST results shifting down towards colder
 540 temperatures with an overall average temperature of 9.60 °C. This would be
 541 more in keeping with the observed SST.

542 5.4. Implications for palaeothermometry

543 One aim of this research was to assess the utility of *S. sachalinensis* as a
 544 palaeothermometer in archaeological studies. As outline in the introduction,
 545 the importance of marine diet over the past 7000 years of Hokkaido’s history

546 means that marine carbonates are a common element of archaeological as-
547 semblages, and the unique hunter-gatherer development in Hokkaido means
548 that there are gaps in our palaeoenvironmental understanding of this region
549 as compared to much of the rest of Japan,

550 In terms of carbon isotopes, our results show a slight but statistically in-
551 significant covariance between high $\delta^{18}\text{O}_{\text{shell}}$ /low $\delta^{13}\text{C}_{\text{shell}}$, with slightly higher
552 $\delta^{13}\text{C}_{\text{shell}}$ values in summer and autumn potentially related to primary pro-
553 ductivity. However, due to the lack of clear seasonal cycling and the complex
554 relationship between $\delta^{13}\text{C}_{\text{shell}}$, oceanography and climate in similar species,
555 we can't currently suggest a way that $\delta^{13}\text{C}_{\text{shell}}$ in *S. sachalinensis* can be
556 employed as an effective subannual palaeoclimatic indicator.

557 By contrast, there is a strong case for the use of stable isotope analy-
558 sis on *S. sachalinensis* as a palaeothermometer. Clear cyclicity can be seen
559 in $\delta^{18}\text{O}_{\text{shell}}$, and based on comparison to observed SST and the position of
560 growth lines, we are confident that ambient water temperature is the main
561 driver. $\delta^{18}\text{O}_{\text{shell}}$ therefore has the potential to provide information on annual
562 and sub-annual climate which should add important climatic and oceano-
563 graphic context to the archaeological record.

564 However, as previously discussed and as expected for proxies of this kind,
565 $\delta^{18}\text{O}_{\text{shell}}$ in this species does not necessarily appear to record the complete
566 annual range of SST. There are a number of factors relating to the specific
567 growth conditions, local oceanography and sample treatment that should be
568 considered as far as possible within a palaeoclimatic or archaeological con-
569 text. For example, exact specimen growth depth will always be an unknown
570 quantity when dealing with archaeological material, but assuming a relatively
571 consistent depth range of 1-15 m for *S. sachalinensis* as well as the fact that
572 prehistoric gatherers would have been more likely to collect preferentially at
573 shallow depths, this uncertainty can be fairly well constrained.

574 The growth pattern of the species, with rapid growth allowing suban-
575 nual incremental sampling until eight to nine years of age, means that *S.*
576 *sachalinensis* could be used to produce a SST proxy at either an inter- or
577 intra-annual resolution. Furthermore, if young, fast-growing, shells are found
578 in an archaeological context it should be possible to use growth-edge sam-
579 ples to estimate season of collection and/or site occupation. This technique
580 was first proposed by Shackleton (1973), and has since been a common fea-
581 ture of stable isotope research in archaeomalacology (e.g. Bosch et al., 2018;
582 Burchell et al., 2013; Jew et al., 2013; Mannino et al., 2007). However, it
583 relies on fast-growing increments at the shell edge so would only be appropri-

ate for archaeological *S. sachalinensis* ontogenetically younger than ~eight years. Given archaeological biases towards larger, more meat-rich specimens, suitable shells are not likely to be commonly encountered except in cases of local resource over-exploitation.

Clumped isotope measurements as a palaeoclimatic proxy within *Spisula sachalinensis* may be a means to circumvent some of the issues identified here. This approach has been successfully used to provide seasonal climate reconstructions from Cretaceous bivalves (de Winter et al., 2020), and has the benefit of being independent from estimations of past $\delta^{18}\text{O}_{\text{seawater}}$ (Eiler, 2007; Henkes et al., 2013), which we have already noted among the confounding factors of temperature interpretation. This will be especially relevant for prehistoric and deep-time bivalves where historical records of seawater composition can't be relied upon, but could also be useful in cases of extreme seasonal variation in $\delta^{18}\text{O}_{\text{seawater}}$ which can be hard to incorporate into palaeoclimate models.

6. Conclusions

These results confirm the inverse relationship between $\delta^{18}\text{O}_{\text{shell}}$ and SST in *Spisula sachalinensis*, as previously identified for long-lived clam species in other regions, and indicate that shells from Tomakomai form a warm-season growth line. When compared to satellite-recorded SST, $\delta^{18}\text{O}_{\text{shell}}$ -derived temperatures fall within the expected range for the region and show clear seasonal cycling. This demonstrates the potential utility of this species as a SST archive in both modern and palaeoclimatic contexts. Possible biases in this record include sample treatment, growth depth and $\delta^{18}\text{O}_{\text{seawater}}$, but further investigation is required to determine the extent to which these affect SST estimation.

This study also highlights complexities in *S. sachalinensis* growth that suggest the need for caution during macro/microscopic sclerochronological assessment. For example, not only is there evidence for variation in growth line formation both between geographically distant shells (e.g. at the southern or northern limits of distribution) but we have also shown that this variation can occur within a single shell (e.g. the anomalous cool-season line observed in TBMOD1). Given these issues, we suggest that stable oxygen isotope analysis in combination with visual macro- and microscopic assessment of shell growth is the most reliable route to *S. sachalinensis* palaeothermometry.

620 **7. Acknowledgements**

621 This work was supported by a NEIFSC project grant [IP-1944-1119]; and
622 a Clarendon Fund Scholarship. Thanks also to Taena Uemura for her help in
623 arranging access to the samples, and Hilary Sloane for her role in the sample
624 preparation and mass spectrometry process.

625 **References**

- 626 Abe, C., Leipe, C., Tarasov, P.E., Müller, S., Wagner, M., 2016. Spatio-
627 temporal distribution of hunter-gatherer archaeological sites in the
628 Hokkaido region (northern Japan): An overview. *Holocene* 26, 1627–1645.
629 doi:10.1177/0959683616641745.
- 630 Agboola, J.I., Uchimiya, M., Kudo, I., Osawa, M., Kido, K., 2013. Season-
631 ality and environmental drivers of biological productivity on the western
632 hokkaido coast, ishikari bay, japan. *Estuarine, Coastal and Shelf Science*
633 doi:10.1016/j.ecss.2013.03.008.
- 634 Arthur, M.A., Anderson, T.F., Kaplan, I.R., Veizer, J., Land, L.S., 1983a.
635 Stable Isotopes in Sedimentary Geology. SEPM Society for Sedimentary
636 Geology. doi:10.2110/scn.83.10.
- 637 Arthur, M.A., Williams, D.F., Jones, D.S., 1983b. Seasonal temperature-
638 salinity changes and thermocline development in the mid- Atlantic Bight
639 as recorded by the isotopic composition of bivalves. *Geology* 11, 655–659.
640 doi:10.1130/0091-7613(1983)11<655:STCATD>2.0.CO;2.
- 641 Bosch, M.D., Mannino, M.A., Prendergast, A.L., Wesselingh, F.P.,
642 O’Connell, T.C., Hublin, J.J., 2018. Year-round shellfish exploita-
643 tion in the Levant and implications for Upper Palaeolithic hunter-
644 gatherer subsistence. *Journal of Archaeological Science: Reports* 21,
645 1198–1214. URL: <http://dx.doi.org/10.1016/j.jasrep.2017.08.014>,
646 doi:10.1016/j.jasrep.2017.08.014.
- 647 Burchell, M., Hallmann, N., Martindale, A., Cannon, A., Schöne, B.R., 2013.
648 Seasonality and Intensity of Shellfish Harvesting on the North Coast of
649 British Columbia. *Journal of Island and Coastal Archaeology* doi:10.1080/
650 15564894.2013.787566.
- 651 Butler, P.G., Wanamaker, A.D., Scourse, J.D., Richardson, C.A., Reynolds,
652 D.J., 2013. Variability of marine climate on the North Icelandic Shelf
653 in a 1357-year proxy archive based on growth increments in the bi-
654 valve *Arctica islandica*. *Palaeogeography, Palaeoclimatology, Palaeoecol-*
655 *ogy* doi:10.1016/j.palaeo.2012.01.016.

- 656 Craig, H., 1957. Isotopic standards for carbon and oxygen and correction
657 factors for mass-spectrometric analysis of carbon dioxide. *Geochimica et*
658 *Cosmochimica Acta* doi:10.1016/0016-7037(57)90024-8.
- 659 Demaree, G.R., Mikami, T., Tsukahara, T., Zaiki, M., 2013. The meteorological
660 Observations of the "Vereenigde Oost-Indische Compagnie (VOC)" -
661 What can be learned from them? *歴史地理学* 55-5, 99–106.
- 662 Dettman, D.L., Reische, A.K., Lohmann, K.C., 1999. Controls on the stable
663 isotope composition of seasonal growth bands in aragonitic fresh-water
664 bivalves (unionidae). *Geochimica et Cosmochimica Acta* 63, 1049–1057.
665 doi:10.1016/S0016-7037(99)00020-4.
- 666 Eiler, J.M., 2007. "Clumped-isotope" geochemistry - The study of naturally-
667 occurring, multiply-substituted isotopologues. *Earth and Planetary Sci-*
668 *ence Letters* 262, 309–327. doi:10.1016/j.epsl.2007.08.020.
- 669 Emiliani, C., Cardini, L., Mayeda, T., McBurney, C., Tongiorgi, E., 1964.
670 Palaeotemperature analysis of marine molluscs (food refuse) from the site
671 of Arene Candide cave, Italy and the Haua Fteah cave, Cyrenaica, in:
672 Craig, H., Miller, S., Wasserburg, G. (Eds.), *Isotopic and Cosmic Chem-*
673 *istry*. North-Holland Publishing Company, Amsterdam, pp. 133–156.
- 674 Geary, D.H., Brieske, T.A., Bemis, B.E., 1992. The Influence and Interaction
675 of Temperature, Salinity, and Upwelling on the Stable Isotopic Profiles of
676 Strombid Gastropod Shells. *PALAIOS* doi:10.2307/3514797.
- 677 Gillikin, D.P., Lorrain, A., Bouillon, S., Willenz, P., Dehairs, F., 2006.
678 Stable carbon isotopic composition of *Mytilus edulis* shells: relation to
679 metabolism, salinity, $\delta^{13}\text{CDIC}$ and phytoplankton. *Organic Geochemistry*
680 37, 1371–1382. doi:10.1016/j.orggeochem.2006.03.008.
- 681 Golikov, A.N., Scarlato, O.A., 1970. Abundance, dynamics and produc-
682 tion properties of populations of edible bivalves *Mizuhopecten yessoen-*
683 *sis* and *Spisula sachalinensis* related to the problem of organization
684 of controllable submarine farms at the Western shores of the Sea of
685 Japan. *Helgoländer Wissenschaftliche Meeresuntersuchungen* 20, 498–513.
686 doi:10.1007/BF01609925.

- 687 Goodwin, D.H., Schöne, B.R., Dettman, D.L., Goodwin, D.H., Schone, B.R.,
688 Dettman, D.L., 2003. Resolution and Fidelity of Oxygen Isotopes as Pale-
689 otemperature Proxies in Bivalve Mollusk Shells: Models and Observations.
690 SEPM Society for Sedimentary Geology 18, 110–125.
- 691 Göttsche, F., Olesen, F.S., 2017. Fiducial Reference Measurements for Vali-
692 dation of Surface Temperature from Satellites (FRM4STS) Technical Re-
693 port 3: A Framework to Verify the Field Performance of TIR FRM. Eu-
694 ropean Space Agency Technical Reports 3.
- 695 Grossman, E.L., Ku, T.L., 1986. Oxygen and carbon isotope fractionation
696 in biogenic aragonite: Temperature effects. *Chemical Geology: Isotope*
697 *Geoscience Section* 59, 59–74. doi:10.1016/0168-9622(86)90057-6.
- 698 Habu, J., Matsui, A., Yamamoto, N., Kanno, T., 2011. Shell mid-
699 den archaeology in Japan: Aquatic food acquisition and long-term
700 change in the Jomon culture. *Quaternary International* 239, 19–
701 27. URL: <http://dx.doi.org/10.1016/j.quaint.2011.03.014>, doi:10.
702 1016/j.quaint.2011.03.014.
- 703 Henkes, G.A., Passey, B.H., Wanamaker, A.D., Grossman, E.L., Ambrose,
704 W.G., Carroll, M.L., 2013. Carbonate clumped isotope compositions of
705 modern marine mollusk and brachiopod shells. *Geochimica et Cosmochim-*
706 *ica Acta* 106, 307–325. URL: [http://dx.doi.org/10.1016/j.gca.2012.](http://dx.doi.org/10.1016/j.gca.2012.12.020)
707 12.020, doi:10.1016/j.gca.2012.12.020.
- 708 Hirose, N., ichi Fukudome, K., 2006. Monitoring the Tsushima warm current
709 improves seasonal prediction of the regional snowfall. *Scientific Online*
710 *Letters on the Atmosphere* 2, 61–63. doi:10.2151/sola.2006-016.
- 711 Hudson, M.J., 2014. The Ethnohistory and Anthropology of ‘Modern’
712 Hunter-Gatherers: North Japan (Ainu), in: Cummings, V., Jordan, P.,
713 Zvelebil, M. (Eds.), *The Oxford Handbook of the Archaeology and An-*
714 *thropology of Hunter-Gatherers*. Oxford University Press.
- 715 Imada, Y., Maeda, S., Watanabe, M., Shiogama, H., Mizuta, R., Ishii, M.,
716 Kimoto, M., 2017. Recent enhanced seasonal temperature contrast in
717 Japan from large ensemble high-resolution climate simulations. *Atmo-*
718 *sphere* 8, 1–13. doi:10.3390/atmos8030057.

- 719 Jew, N.P., Erlandson, J.M., Rick, T.C., Watts, J., 2013. Shellfish, Sea-
720 sonality, and Sedentism: $\delta^{18}\text{O}$ Analysis of California Mussels from Early
721 Holocene Shell Middens on San Miguel Island, California. *Pacific Archae-*
722 *ology* 4.
- 723 Jones, D.S., Williams, D.F., Arthur, M.A., 1983. Growth history and ecology
724 of the Atlantic surf clam, *Spisula solidissima* (Dillwyn), as revealed by sta-
725 ble isotopes and annual shell increments. *Journal of Experimental Marine*
726 *Biology and Ecology* 73, 225–242. doi:10.1016/0022-0981(83)90049-7.
- 727 Kato, Y., Hamai, I., 1975. Growth and Shell Formation of the Surf Clam,
728 *Spisula sachalinensis* (Schrenck). *Bulletin of the Faculty of Fisheries,*
729 *Hokkaido University* 25, 291–303.
- 730 Khim, B.K., Woo, K.S., Je, J.G., 2000. Stable isotope profiles of bivalve
731 shells: Seasonal temperature variations, latitudinal temperature gradients
732 and biological carbon cycling along the east coast of Korea. *Continental*
733 *Shelf Research* 20, 843–861. doi:10.1016/S0278-4343(00)00004-2.
- 734 Kinoshita, T., Shibuya, S., 1920. Muroran oyobi Kamiiso san hokkigai no
735 sanranki. *Hokusuisi Jumbo* 4-5.
- 736 Kodaira, T., Horikawa, K., Zhang, J., Senjyu, T., 2016. 日本海対馬暖
737 流域における海水の酸素同位体比と塩分の関係 (relationship between
738 seawater oxygen isotope ratio and salinity in the tsushima current, the
739 sea of japan). *Chikyukagaku (Geochemistry)* 50, 263–277. doi:10.14934/
740 *chikyukagaku*.50.263.
- 741 Können, G.P., Zaiki, M., Baede, A.P., Mikami, T., Jones, P.D., Tsukahara,
742 T., 2003. Pre-1872 extension of the Japanese instrumental meteorological
743 observation series back to 1819. *Journal of Climate* 16, 118–131. doi:10.
744 1175/1520-0442(2003)016<0118:PEOTJI>2.0.CO;2.
- 745 Krantz, D.E., Williams, D.F., Jones, D.S., 1987. Ecological and pa-
746 leoenvironmental information using stable isotope profiles from living
747 and fossil molluscs. *Palaeogeography, Palaeoclimatology, Palaeoecology*
748 doi:10.1016/0031-0182(87)90064-2.
- 749 Lee, J.Y., Chang, Y.J., Park, Y.J., 1996. Spawning Induction and Egg
750 Development of Surf Clam, *Spisula sachalinensis*. *Journal of Aquaculture*
751 (한국양식학회지) 9, 419–427.

- 752 Leng, M.J., Lewis, J.P., 2016. Oxygen isotopes in Molluscan shell: Ap-
753 plications in environmental archaeology. *Environmental Archaeology* 21,
754 295–306. doi:10.1179/1749631414y.0000000048.
- 755 Li, X., 2017. Study on stable isotopes of precipitation in Hokkaido, North
756 Japan. Ph.D. thesis. doi:10.14943/doctoral.r7033.
- 757 Loftus, E., Rogers, K., Lee-Thorp, J., 2015. A simple method to estab-
758 lish calcite: Aragonite ratios in archaeological mollusc shells. *Journal of*
759 *Quaternary Science* 30, 731–735. doi:10.1002/jqs.2819.
- 760 Makino, M., 2011. Fisheries Management in Japan: Its institutional features
761 and case studies. doi:10.1007/978-94-007-1777-0.
- 762 Mann, R., Munroe, D., Powell, E., Hofmann, E., Klinck, J., 2013. Bi-
763 valve Molluscs: Barometers of Climate Change in Arctic Marine Systems,
764 in: Mueter, F., Dickson, D., Huntingdon, H., Irvine, J., Logerwell, E.,
765 MacLean, S., Quakenbush, L., Rosa, C. (Eds.), *Responses of Arctic Ma-*
766 *rine Ecosystems to Climate Change*. University of Alaska Fairbanks, pp.
767 61–82. doi:10.4027/ramecc.2013.04.
- 768 Mannino, M.A., Thomas, K.D., Leng, M.J., Piperno, M., Tusa, S., Taglia-
769 cozzo, A., 2007. Marine resources in the mesolithic and neolithic at the
770 Grotta dell’Uzzo (Sicily): Evidence from isotope analyses of marine shells.
771 *Archaeometry* 49, 117–133. doi:10.1111/j.1475-4754.2007.00291.x.
- 772 Marullo, S., Minnett, P., Santoleri, R., Tonani, M., 2016. The Diurnal Cycle
773 of Sea-Surface Temperature and Estimation of the Heat Budget of the
774 Mediterranean Sea. *Journal of Geophysical Research: Oceans* 121, 6762–
775 6778. doi:10.1002/2016JC012132.Received.
- 776 McConnaughey, T.A., Gillikin, D.P., 2008. Carbon isotopes in mol-
777 lusk shell carbonates. *Geo-Marine Letters* 28, 287–299. doi:10.1007/
778 s00367-008-0116-4.
- 779 Mikami, T., 2008. Climatic variations in Japan reconstructed from historical
780 documents. *Weather* 63, 190–193. doi:10.1002/wea.281.
- 781 Milano, S., Prendergast, A.L., Schöne, B.R., 2016. Effects of cooking on mol-
782 lusk shell structure and chemistry: Implications for archeology and pale-
783 oenvironmental reconstruction. *Journal of Archaeological Science: Reports*

784 7, 14–26. URL: <http://dx.doi.org/10.1016/j.jasrep.2016.03.045>,
785 doi:10.1016/j.jasrep.2016.03.045.

786 Moon, L.R., Judd, E.J., Thomas, J., Ivany, L.C., 2018. Out of the oven and
787 into the fire: Unexpected preservation of the seasonal $\delta^{18}\text{O}$ cycle following
788 heating experiments on shell carbonate. *Palaeogeography, Palaeoclimatology,*
789 *Palaeoecology* 532.

790 Müller, P., Staudigel, P.T., Murray, S.T., Vernet, R., Barusseau, J.P.,
791 Westphal, H., Swart, P.K., 2017. Prehistoric cooking versus accurate
792 palaeotemperature records in shell midden constituents. *Scientific Reports*
793 doi:10.1038/s41598-017-03715-8.

794 Nagasaki, F., 1994. Beef-eating culture and fish-eating culture.
795 Nousangyoson-bunka-kyokai, Tokyo.

796 Noh, Y., Lee, E., Kim, D.H., Hong, S.Y., Kim, M.J., Ou, M.L., 2011.
797 Prediction of the diurnal warming of sea surface temperature using an
798 atmosphere-ocean mixed layer coupled model. *Journal of Geophysical Re-*
799 *search: Oceans* 116, 1–15. doi:10.1029/2011JC006970.

800 Ohnuki-Tierney, E., 1976. Regional Variations in Ainu culture. *American*
801 *Ethnologist* 3, 297–329. URL: [http://onlinelibrary.wiley.com/doi/](http://onlinelibrary.wiley.com/doi/10.1525/ae.1976.3.2.02a00080/abstract)
802 [10.1525/ae.1976.3.2.02a00080/abstract](http://onlinelibrary.wiley.com/doi/10.1525/ae.1976.3.2.02a00080/abstract), doi:10.1525/ae.1976.3.2.
803 02a00080.

804 Oikawa, A., 1995. Kaizuka database no suryo-teki bunseki. (Quantitative
805 analysis of shell-mound database). *Jinbun Kagaku to Computer (Human-*
806 *ities and Computer)* 25, 59–66.

807 Okada, H., 1998. Maritime Adaptations in Northern Japan. *Arctic Anthro-*
808 *pology* 35, 335–339. URL: [http://muse.jhu.edu/content/crossref/](http://muse.jhu.edu/content/crossref/journals/asian{}_perspectives/v045/45.1matsumura.pdf)
809 [journals/asian{}_perspectives/v045/45.1matsumura.pdf](http://muse.jhu.edu/content/crossref/journals/asian{}_perspectives/v045/45.1matsumura.pdf).

810 Sakaizawa, R., Kawai, T., Sato, T., Oyama, H., Tsumune, D., Tsubono,
811 T., Goto, K., 2018. The inclusion of ocean-current effects in a tidal-
812 current model as forcing in the convection term and its application to
813 the mesoscale fate of CO₂ seeping from the seafloor. *Ocean Modelling*
814 123, 40–54. URL: <https://doi.org/10.1016/j.ocemod.2018.01.001>,
815 doi:10.1016/j.ocemod.2018.01.001.

- 816 Sakurai, I., Miyamoto, T., Kurata, M., 1992. Breeding season of the Japanese
817 surf clam *Pseudocardium sybilla* in Tomakomai and Shizunai, southwest
818 Hokkaido. Scientific Reports of the Hokkaido Fisheries Experimental Sta-
819 tion 39, 45–52.
- 820 Sakurai, I., Seto, M., 1998. Behavioral Characteristics of the Juvenile
821 Japanese Surf Clam *Pseudocardium sachalinensis* in response to Sand Ero-
822 sion and Deposition Associated with Oscillatory Water Flow. Fisheries
823 Science 64, 367–372.
- 824 Sasaki, K., 1981. Growth of the Sakhalin Surf Clam, *Spisula sachalinensis*
825 (SCHRENCK), in Sendai Bay. Tohoku Journal of Agricultural Research
826 32, 168–180.
- 827 Sasaki, K., 1989. Characteristics of the Bottom Sediments Inhabited by the
828 Surf Clam *Spisula sachalinensis* in Sendai Bay. Nippon Suisan Gakkaishi
829 55, 1127–1131.
- 830 Sasaki, S., Ohta, T., 1999. Seasonal variation of chemical components in surf
831 clam (*Spisula sachalinensis*). Food Sci.Technol.Res. 5, 313–315.
- 832 Schmidt, G.A., Bigg, G.R., Rohling, E.J., 1999. Global Seawater Oxygen-18
833 Database - v1.22. URL: <https://data.giss.nasa.gov/o18data/>.
- 834 Schöne, B.R., 2008. The curse of physiology - Challenges and opportunities
835 in the interpretation of geochemical data from mollusk shells. Geo-Marine
836 Letters 28, 269–285. doi:10.1007/s00367-008-0114-6.
- 837 Schöne, B.R., Fiebig, J., Pfeiffer, M., Gleß, R., Hickson, J., Johnson,
838 A.L., Dreyer, W., Oschmann, W., 2005. Climate records from a bi-
839 valved Methuselah (*Arctica islandica*, Mollusca; Iceland). Palaeogeog-
840 raphy, Palaeoclimatology, Palaeoecology 228, 130–148. doi:10.1016/j.
841 palaeo.2005.03.049.
- 842 Seaton, P., 2017. Japanese Empire in Hokkaido. URL:
843 [http://asianhistory.oxfordre.com/view/10.1093/acrefore/](http://asianhistory.oxfordre.com/view/10.1093/acrefore/9780190277727.001.0001/acrefore-9780190277727-e-76)
844 [9780190277727.001.0001/acrefore-9780190277727-e-76,](http://asianhistory.oxfordre.com/view/10.1093/acrefore/9780190277727.001.0001/acrefore-9780190277727-e-76)
845 [doi:10.1093/acrefore/9780190277727.013.76.](http://asianhistory.oxfordre.com/view/10.1093/acrefore/9780190277727.001.0001/acrefore-9780190277727-e-76)

- 846 Selin, N.I., 2010. The growth and life span of bivalve mollusks at the north-
847 eastern coast of Sakhalin Island. *Russian Journal of Marine Biology* 36,
848 258–269. doi:10.1134/S1063074010040048.
- 849 Seo, H., Kwon, Y.O., Park, J.J., 2013. On the effect of the East/Japan Sea
850 SST variability on the North Pacific atmospheric circulation in a regional
851 climate model. *Journal of Geophysical Research* 119, 418–444. doi:10.
852 1038/175238c0.
- 853 Shackleton, N.J., 1973. Oxygen Isotope Analysis as a Means of Determining
854 Season of Occupation of Prehistoric Midden Sites. *Archaeometry* 15, 133–
855 141. doi:10.1111/j.1475-4754.1973.tb00082.x.
- 856 Stuart, C., 2020. Python Script for Extracting SST Data from NOAA
857 Database. URL: <https://github.com/christuart/ghrsst>.
- 858 Tabakaeva, O.V., Tabakaev, A.V., 2017. Lipids and fatty acids from soft
859 tissues of the bivalve mollusk *Spisula Sachalinensis*. *Chemistry of Natural*
860 *Compounds* 53, 16–20. doi:10.1007/s10600-017-1900-z.
- 861 Takahashi, N., Yamamoto, K., 1970. Histological Studies on the Reproduc-
862 tive Cycle of the Surf Clam, *Spisula sachalinensis*. Seasonal Changes in the
863 Ovary. *Bulletin of the Japanese Society of Scientific Fisheries* 36, 345–352.
- 864 Takamaru, N., 1976. On the breeding season of the surf clam, *Spisula sacha-*
865 *linensis* (Schrenk) in Tokachi. *Journal of Hokkaido Fisheries Experimental*
866 *Station* 33, 1–8.
- 867 Takano, Y., Tachibana, Y., Iwamoto, K., 2008. Influences of large-scale
868 atmospheric circulation and local sea surface temperature on convective
869 activity over the sea of Japan in December. *Scientific Online Letters on*
870 *the Atmosphere* 4, 113–116. doi:10.2151/sola.2008-029.
- 871 Twaddle, R.W., Ulm, S., Hinton, J., Wurster, C.M., Bird, M.I., 2016. Sclero-
872 chronological analysis of archaeological mollusc assemblages: methods,
873 applications and future prospects. *Archaeological and Anthropological Sci-*
874 *ences* 8, 359–379. doi:10.1007/s12520-015-0228-5.
- 875 de Winter, N., Müller, I., Kocken, I., Thibault, N., Ullmann, C.V.,
876 Farnsworth, A., Lunt, D., Claeys, P., Ziegler, M., 2020. First absolute

- 877 seasonal temperature estimates for greenhouse climate from clumped iso-
878 topes in bivalve shells. (Preprint) doi:10.21203/rs.3.rs-39203/v1.
- 879 Yamamoto, K., 1947. Hokkigai no seicho ni tsuite. Sapporo nōrin-gakkin-hō
880 (Journal of the Sapporo Society of Agriculture and Forestry) 36, 51–62.